(12) INTERNATIONAL APPLICATION PUBLISHED UNDER THE PATENT COOPERATION TREATY (PCT)

(19) World Intellectual Property Organization
International Bureau

(43) International Publication Date
3 November 2005 (03.11.2005)

PCT

(10) International Publication Number
WO 2005/103798 A2

(51) International Patent Classification[7]: **G02F 1/00**

(21) International Application Number: PCT/US2005/013200

(22) International Filing Date: 12 April 2005 (12.04.2005)

(25) Filing Language: English

(26) Publication Language: English

(30) Priority Data:
60/562,799 14 April 2004 (14.04.2004) US

(71) Applicant *(for all designated States except US)*: **THE GOVERNMENT OF THE UNITED STATES OF AMERICA, as represented by THE SECRETARY OF THE NAVY** [US/US]; Naval Research Laboratory, 4555 Overlook Avenue, SW, Code 1008.2, Washington, DC 20375 (US).

(72) Inventors; and
(75) Inventors/Applicants *(for US only)*: **WILLIAMS, Keith, J.** [US/US]; 12101 Palisades Drive, Dunkirk, MD 20754 (US). **TULCHINSKY, David, A.** [US/US]; 4012 North 26th Street, Arlington, VA 22207 (US).

(74) Agent: KARASEK, John, J.; Associate Counsel (Patents), Naval Research Laboratory, 4555 Overlook Avenue, SW, Washington, DC 20375-5325 (US).

(81) Designated States *(unless otherwise indicated, for every kind of national protection available)*: AE, AG, AL, AM, AT, AU, AZ, BA, BB, BG, BR, BW, BY, BZ, CA, CH, CN, CO, CR, CU, CZ, DE, DK, DM, DZ, EC, EE, EG, ES, FI, GB, GD, GE, GH, GM, HR, HU, ID, IL, IN, IS, JP, KE, KG, KM, KP, KR, KZ, LC, LK, LR, LS, LT, LU, LV, MA, MD, MG, MK, MN, MW, MX, MZ, NA, NI, NO, NZ, OM, PG, PH, PL, PT, RO, RU, SC, SD, SE, SG, SK, SL, SM, SY, TJ, TM, TN, TR, TT, TZ, UA, UG, US, UZ, VC, VN, YU, ZA, ZM, ZW.

(84) Designated States *(unless otherwise indicated, for every kind of regional protection available)*: ARIPO (BW, GH, GM, KE, LS, MW, MZ, NA, SD, SL, SZ, TZ, UG, ZM, ZW), Eurasian (AM, AZ, BY, KG, KZ, MD, RU, TJ, TM), European (AT, BE, BG, CH, CY, CZ, DE, DK, EE, ES, FI, FR, GB, GR, HU, IE, IS, IT, LT, LU, MC, NL, PL, PT, RO, SE, SI, SK, TR), OAPI (BF, BJ, CF, CG, CI, CM, GA, GN, GQ, GW, ML, MR, NE, SN, TD, TG).

Published:
— *without international search report and to be republished upon receipt of that report*

For two-letter codes and other abbreviations, refer to the "Guidance Notes on Codes and Abbreviations" appearing at the beginning of each regular issue of the PCT Gazette.

(54) Title: PHOTONIC MICROWAVE AMPLIFIER

(57) Abstract: An apparatus including an impedance matching circuit, a biasing circuit, and a number of serially connected optically controlled current sources for detecting amplitude-modulated light at RF frequencies. The serially connected optically controlled current sources are connected to the impedance matching circuit and to the biasing circuit. Optionally, the biasing circuit applies a respective bias voltage to each of the serially connected optically controlled current sources.

WO 2005/103798 A2

PHOTONIC MICROWAVE AMPLIFIER

Technical Art

The invention relates generally to amplifiers, and more specifically to high power, high linearity, photonic microwave amplifiers.

Background Art

A fiber optic link is shown in FIG. 1. A RF-to-Optical converter 10 takes, as an input, electrical RF signal and impresses it upon an optical carrier 20. For example, the optical carrier includes one or more delays and an optical amplifier or other optical processor. This can be accomplished with various modulation techniques including, for example, intensity, amplitude, phase, polarization, or frequency modulation. Once the electrical or RF signal resides on an optical carrier 20, it can be remoted with minimal signal loss using an optical fiber, amplified with the optical amplifier, optically processed, and delivered to an Optical-to-RF converter 30, which converts the modulated light signal back into the electrical domain. This type of link can be described as a black box with a RF input and a RF output as if it were any "two port electrical network." The gain, noise figure, output power, third order intercept, and/or other linear and nonlinear characteristics can be fully characterized.

Some of the highest linearity and most common photonic links utilize external modulators with continuous wave ("CW") lasers as the RF-to-Optical converters. A popular, external modulator is a LiNbO3 Mach-Zehnder modulator ("MZM"). An example of a Y-branched MZM is shown in FIG. 2. The input light to the MZM in FIG. 2 is split at the input Y-branch. The two parallel optical waveguide arms act as two phase modulators, which can operate in a push-pull manner when driven by an external electric field, such as an RF input signal. The phase modulation is made possible due to the electro-optic properties of the $LiNbO_3$, in which the velocity of the light is proportional to the externally applied electric field. The light from the upper waveguide path is recombined with the light from the lower path at the output Y-branch. If the two optical beams arrive in phase, the light will be guided out of the modulator. If the two beams are out of phase, the light will not be guided out of the MZM. Thus, a MZM can be used to produce a transmission loss, dependent upon the applied electric field. The optical output from a MZM depends sinusoidally on the input electrical signal as shown in FIG. 3. The overall performance of a MZM is characterized by the switching voltage, V_{pi}, which is the difference in bias voltages at the minimum and maximum transmission points. For linearity and maximum differential change in optical output signal per input volt, the modulator is typically biased at the point at which the output is one-half of the maximum output signal. This point in the MZM transfer function is called quadrature and is typically accomplished by applying an external bias voltage. When biased at quadrature, the modulator optical output signal P_{out} is given by,

$$P_{out} = \frac{P_{in}}{2}(1 \pm \sin(kx)) + P_{minimum} \quad (0)$$

where P_{in} is the input optical power, k is a constant, x is the input signal voltage, $P_{minimum}$ is the minimum optical transmission of the modulator, and the sign (±) depends on the slope of the quadrature point chosen.

When the input signal, x, is a time-varying sinusoid, the output is a sinusoid with a sinusoidal argument. The resulting output can be expressed as a Fourier series with coefficients or weights of the Bessel function form. The magnitude of the coefficients represents the magnitude of the linear (i.e., first non-DC term) and nonlinear (i.e., higher order terms) output signals. The maximum linear term (i.e., the fundamental frequency) of the response is 3.9 dB down from the maximum linear response, namely, 100% modulation depth, when the fundamental output is at saturation (i.e., maximum possible fundamental output) as described by A. Katz, W. Jemison, M. Kubak, and J. Dragone, "Improved Radio Over Fiber Performance Using Predistortion Linearization," IEEE MTT-S Digest, paper IFWE-53, p. 1403, 2003, incorporated herein by reference. This characteristic of the MZM transfer function will be a limitation for generating maximum linear power from the Optical-to-RF converter described in this invention. It may therefore be useful to consider one of the other many ways to implement the RF-to-Optical converter.

As represented in FIGs. 4a-4c, photodiodes, the main component in the Optical-to-RF converter, respond to optical intensity and not optical phase. FIG. 4a shows an example of a RF amplitude modulated lightwave carrier input to the Optical-to-RF converter 40 in FIG. 4b. The Optical-to-RF converter 40 outputs a RF envelope output, such as, shown illustratively in FIG. 4c. Optical photodetectors, being square law devices, take the incident optical field(s) and square them, resulting in an output electrical RF signal that is the intensity "envelope" of the optical wave.

Other examples of RF-to-Optical converter configurations, which produce intensity modulated lightwaves, include optical heterodyne systems, directly modulated laser diodes, single-sideband ("SSB") modulated lasers, electroabsorption modulated ("EAM") implementations, all of which RF-to-Lightwave converters can provide the necessary intensity modulated lightwave for a photodetector to demodulate.

There are also many optical phase encoded modulation implementations of RF-to-Lightwave converters. Ultimately though, it will be necessary to provide an amplitude (or intensity) modulated signal to the Optical-to-RF converter. The conversion of other modulation formats, such as phase or polarization modulation, into amplitude modulation can be performed in many ways. The demodulation of phase encoded modulation can be accomplished with, for example, either of two types of phase modulated light demodulators including an optical MZM with a differential delay line within the interferometer to convert an optical phase modulation into an intensity modulation ("Homodyne") and a heterodyne demodulator where an optical local oscillator ("LO") is used to convert phase to intensity modulation. Coherent homodyne detection is a common technique in digital DPSK receivers, such as discussed in A. Knauck X. Liu, X. Wei, D. Gill, and E. Burrows, " Comparison of Modulation Formats for 42.7 Gb/s Single-Channel Transmission Through 1980 km of SSMF," *IEEE Photon. Tech. Lett.*, vol. 16, no. 3, pp. 909, 2004, incorporated herein by reference. Using coherent homodyne detection, digital information is impressed on an Optical carrier with differential phase shift keyed (DPSK) encoding. A polarization demodulation technique utilizes a polarization analyzer to decode polarization (a particular form of optical phase modulation) into intensity modulation.

Disclosure of the Invention

An embodiment of the invention includes an apparatus comprising an impedance matching circuit; a biasing circuit; and a plurality of serially connected optically controlled current sources for detecting amplitude-modulated light at RF frequencies, the plurality of serially connected optically controlled current sources connected to the impedance matching circuit and to the biasing circuit.

Optionally, the apparatus further comprises a plurality of voltage drift prevention circuits connected the plurality of serially connected optically controlled current sources. Optionally, the biasing circuit comprises a bias voltage, and each voltage drift prevention circuit of the plurality of voltage drift prevention circuits comprises an inductor and a fractional voltage of the bias voltage connected thereto. Optionally, the biasing circuit applies a respective bias voltage to each optically controlled current source of the plurality of serially connected optically controlled current sources. Optionally, the biasing circuit comprises a plurality of passive electrical components.

Optionally, the apparatus further comprises a transmission line imbedded in which are the plurality of optically controlled current sources; and a plurality of impedances corresponding to each of the plurality of optically controlled current sources.

Optionally, the apparatus further comprises at least one of a laser and an optical amplifier communicating with the plurality of serially connected optically controlled current sources.

Optionally, each of the plurality of optically controlled current sources comprises at least one of a photodetector, a photoconductive switch, and an avalanche photodiode.

Another embodiment of the invention includes an apparatus comprising an impedance matching circuit; a biasing circuit; and a plurality of parallel, optically controlled current source arrays, each optically controlled current source array of the plurality of parallel, optically controlled current source arrays being connected to the impedance matching circuit and to the biasing circuit, the each optically controlled current source array of the plurality of parallel, optically controlled current source arrays comprising a plurality of serially connected optically controlled current sources for detecting amplitude-modulated light at RF frequencies.

Optionally, the apparatus further comprises a transmission line imbedded in which are said plurality of optically controlled current sources; and a plurality of impedances corresponding to each of said plurality of optically controlled current sources.

Another embodiment of the invention includes an apparatus comprising a first impedance matching circuit; a first biasing circuit; and a first plurality of parallel, optically controlled current source arrays, each optically controlled current source array of the first plurality of parallel, optically controlled current source arrays being connected to the first impedance matching circuit and to the biasing circuit, the each optically controlled current source array of the first plurality of parallel, optically controlled current source arrays comprising a first plurality of serially connected optically controlled current sources for detecting amplitude-modulated light at RF frequencies. The apparatus also includes a second biasing circuit comprising an opposite voltage polarity relative to the first biasing circuit; and a second plurality of parallel, optically controlled current source arrays connected to the first impedance matching circuit, each optically controlled current source array of the second plurality of parallel, optically controlled current source arrays being connected to said first impedance matching circuit and to the biasing circuit, the each optically controlled current source array of the second plurality of parallel, optically controlled current source arrays comprising a second plurality of serially connected optically controlled current sources for detecting amplitude-modulated light at RF frequencies.

Optionally, the first biasing circuit applies a respective bias voltage to each optically controlled current source of said first plurality of serially connected optically controlled current sources, and the second biasing circuit applies a respective bias voltage to each optically controlled current source of said second plurality of serially connected optically controlled current sources.

Optionally, the apparatus further comprises a transmission line imbedded in which are the plurality of optically controlled current sources; and a plurality of impedances corresponding to each of the plurality of optically controlled current sources.

An embodiment of the invention described herein delivers high RF powers directly from photodetectors and photodetector arrays. An embodiment of this invention provides for substantial power gain in fiber-optic signal processing and communications systems and potentially radar arrays. An embodiment of this invention also makes possible the operation of remoted RF power sources without remoted electric biasing (photovoltaic photodetector operation) for low RF power output systems. An embodiment of this invention implements high frequency and bandwidth power amplifiers with high efficiency. An embodiment of this invention is compatible with existing RF-to-Lightwave converters. An embodiment of this invention allows for the possibility to remote high power microwave signals with very little transmission loss.

Embodiments of this invention have a wide variety of government and commercial applications. Examples of such applications include uses as optical oscillators, high dynamic range microwave photonic links, high resolution analog-to-digital converters, frequency down converters for radar, cells sites, and phased arrays for space-based communications.

Brief Description of the Drawings

FIG. 1 is a block diagram of a fiber optic link.

FIG. 2 is a schematic of a Mach Zehnder modulator.

FIG. 3 is an illustrative graph of optical output from a typical Mach Zehnder modulator.

FIG. 4a is an illustrative RF amplitude modulated lightwave carrier.

FIG. 4b is an illustrative optical-to-RF converter having a photodetector receiving the RF amplitude modulated lightwave carrier of FIG. 4a and a load impedance.

FIG. 4c is an illustrative RF envelope output seen at the load impedance of FIG. 4b.

FIG. 5 is an illustrative block diagram of an optimized single photodetector output stage according to an embodiment of the instant invention.

FIG. 6 is an illustrative block diagram of internal equivalent circuit of the output stage of FIG. 5.

FIG. 7 is an illustrative graph of RF power output and efficiency of the output stage of FIG. 5, using a 100 micron diameter photodetector.

FIG. 8 is an illustrative graph of the power conversion efficiency of the output stage of FIG. 5.

FIG. 9 is a set of illustrative time-aligned graphs of oscilloscope traces of output stage of FIG. 5.

FIG. 10 is an illustrative graph of RF power output stage, using a 34 micron diameter photodetector.

FIG. 11 is an illustrative block diagram of an output stage having series-connected photodetectors according to an embodiment of the invention.

FIG. 12 is an illustrative block diagram of an internal equivalent circuit of the output stage of FIG. 11.

FIG. 13 is an illustrative graph of the power conversion efficiency of the output stage of FIG. 11.

FIG. 14 is an illustrative block diagram of a voltage drift prevention circuit according to an embodiment of the invention.

FIG. 15 is an illustrative graph of the RF response for two series connected photodetectors according to an embodiment of the invention.

FIG. 16 is an illustrative block diagram of a traveling wave configuration using three photodetectors according to an embodiment of the instant invention.

FIG. 17 is an illustrative block diagram of a two dimensional photodetector array according to an embodiment of the instant invention.

FIG. 18 is an illustrative block diagram of a two dimensional, balanced, lumped element photodetector array according to an embodiment of the invention, optionally for high output RF power and noise balancing.

Description of the Preferred Embodiments of the Invention

An embodiment of the invention includes an all photonic RF amplifier that can serve as the Optical-to-RF converter 10 in FIG. 1. Such an embodiment, for example, overcomes the output RF power limitations from conventional photodetectors. An embodiment of the invention includes, for example, 1) a optimized high-current high-voltage single photodetector optimally designed to deliver the maximum current and maximum voltage simultaneously into, for example, 50 ohms or other representative output impedance the subsequent RF circuit contains, 2) a series combination of low voltage, high current photodetectors, which effectively increases the maximum voltage possible from photodetector output stages, and which, in an embodiment of the invention, provides for a more intrinsically optimally matched impedance for low voltage standing wave ratio ("VSWR") matching without the addition of external impedance matching circuits which either limit bandwidth or reduce efficiency, and/or 3) a series and parallel combination of single photodetectors for achieving extremely high output power scaling. The last 2 areas, (2) and (3), are, for example, accomplished either in a lumped element circuit configuration for low frequency operation or in a traveling wave circuit configuration for higher frequency operation. An optional enhancement of the lumped element and/or traveling wave circuit configurations, for example, combines diodes as differentially balanced push/pull diode pairs. In addition to the higher output RF power that a balance pair produces, the optional balanced configuration incorporates the noise balancing properties of differential pairs.

The noise figure, gain, linearity, and total efficiency of the amplifier in FIG. 1 are governed by the overall link design and the choice of the particular RF-to-Optical converter and laser/optical amplifier utilized. The performance of the amplifier in these aspects, for example, performs at least as well as the RF counterparts and potentially much better.

Conventional single photodetectors are not designed to provide for an optimal match between the output impedances of, for example, 50 ohms or higher due to the limitations on the applied voltage biases and the loading of the RF power delivered to the load causing a reduction in applied bias voltage. An embodiment of the invention implements class A, AB and/or B output stages which overcomes these limitations. FIG. 5 shows a block diagram of an optimized single photodetector output stage 50 according to an embodiment of the instant invention. For example, a reversed biased photodetector 60 (negative voltage biased by voltage source 45 having voltage Vbias through inductor 70 having inductance L) is connected to an optional impedance matching network, such as one containing series impedance 80 and parallel impedance 90 through a DC blocking capacitor 100 having capacitance C, located either before and/or after the impedance matching network, connected to the load impedance 110 which is, for example, 50 ohms, without loss of generality. Generally, the inductance L is chosen such that the inductor 70 passes the DC current and voltage but which provides a high impedance (i.e., a block) throughout the RF operation frequency range of the output stage 50. Generally, a value of capacitance C is chosen such that the capacitor 100 blocks the DC current and voltage but which provides a low impedance (i.e., a short) throughout the RF operation frequency range of the output stage 50.

From the RF viewpoint over which the output stage delivers RF current and voltage to the load impedance, the photodetector internal equivalent circuit 120 for the photodetector output stage 50 of FIG. 5 is shown in FIG. 6. The photodetector 60 is treated as an ideal current source 130 with current Ipd, as well as with capacitor 140 having capacitance Cpd and resistor 150 having resistance Rpd representing the internal junction capacitance and the series impedance of the photodetector 60, respectively. By way of example, typical photodetector shunt resistance is above 1 Kohm to 10 Kohms and can be neglected for RF (e.g., 50 ohm) systems. Series impedance 80 and parallel impedance 90 are the optionally added external impedance matching elements. Their values (that is, amplitude and phase in the case of capacitive or inductive matching) are determined by the acceptable impedance matching requirements afforded by the particular application. Of particular issue is the acceptable VSWR required to maintain low frequency response ripple, RF phase response over frequency, and/or damage imposed on the output stage (a common problem for RF power amplifiers) due to reflected power back into the output stage. Alternatively, there may be other system-related reasons for choosing a particular impedance match.

For the optimization method for design for power delivery operation, the photodetectors need to be designed such that they simultaneously reach their maximum rated photocurrent (Imax) and maximum output voltage (Vmax). This occurrence results in the detector delivering maximum output power to a given external load impedance (Rload). To determine the optimal photodetector design for a given Rload and a given impedance matching circuit Zs and Zp (as in FIG. 6) the following equation (1) gives the relationship between Imax and Vmax:

$$V_{max} = I_{max}\left(\frac{R_{load}Z_p}{R_{load}+Z_p} + R_{pd} + Z_s\right) \qquad (1)$$

The sum of the terms within the parentheses above is the net load impedance seen by the ideal current source 130 of the photodetector 60.

As an example of the performance of such an output stage, measurements highlighting the baseline performance of this invention are as follows. Utilizing a high current photodetector of the type described in X. Li, S. Demiguel, N. Li, J. Campbell, D. Tulchinsky and K. Williams, " Backside Illuminated High Saturation Current Partially Depleted Absorber Photodetectors," *Electronics Lett.*, v. 39, p. 1466, 2003, incorporated herein by reference, large-signal output power measurements are, for example, made with the biasing arrangement outlined in FIG. 5 without the series impedance 80 (i.e., a short circuit) and parallel impedance 90 (i.e., open circuit). By way of illustration, a 100% modulation depth signal from the output of a phase-locked pair of lasers illuminated a 100μm and a separate 34μm photodetector at offset locking frequencies of 100 MHz and 2 GHz, respectively.

As an example, the data for a 100 micron diameter photodetector at 100MHz is shown in FIG. 7. The incident light level was fixed at 153 mW and the applied bias voltage was increased from 0 to 6.5 Volts reverse bias. The detected photocurrent varied due to space-charge-related compression at lower applied biases, but at 5V was about 130 mA. At each bias level, the output RF power was measured from the photodetector into the 50 ohm load of an RF power meter. The output RF power was measured and plotted against the total power (optical + electrical) input to the stage. The electrical power input to the photodetector is just the power delivered by the power supply providing the bias voltage and is equal to the average photocurrent multiplied by the bias voltage. As can be seen in FIG. 7, the output RF power increases with applied bias voltage until total input powers exceed 900 mW (about 6 volt bias). The resulting efficiency peaks at around 45% and decreases to 30% at the highest applied voltage.

$$V_{\text{bias, min}} = V_{\text{pk-load}} + \frac{2I_{\text{ave}}}{\alpha} + V_{\text{th}} \qquad (2)$$

Equation (2) above outlines the minimum bias voltage required to maintain class A operation from the photodetector. For a 100% modulation depth, 130 mA average photocurrent from this photodetector (alpha = 0.17A/V and Vth=-0.4V), Vbias,min = (0.13*50 + 2*0.13/0.17 –0.4V) = 7.6 Volts. However, the maximum applied voltage in FIG. 7 is only 6.5 V. Therefore, the data in FIG. 7 represents class AB operation where significant clipping of the peak voltage across the load impedance is occurring. In addition, this photodetector at these high powers optionally experiences, for example, thermal issues, which may also be responsible for a small drop in efficiency.

$$\eta = \frac{1}{\left(2 + \frac{4}{\alpha R} + \frac{2V_{th}}{V_{pk-load}} + \frac{P_{\text{abs}}}{P_{\text{load}}}\right)} \qquad (3)$$

To compare these efficiencies to that which is theoretically obtainable from equation (3) above, FIG. 8 shows a plot of equation (5) with a =0.17 A/V and Vth = -0.4V along with the plot with alpha infinite (ideal) and Vth=0. As can be seen, for a +24 dBm output stage, efficiencies in the 36% range are achieved when the photodetector is biased exactly with the minimum applied bias for class A operation. From FIG. 7, 30% is achieved at the highest bias, in reasonable agreement with the calculation. At lower applied voltages, higher efficiencies are achieved, but this again is when the photodetector is operating in class AB operation.

To verify class AB operation, FIG. 9 shows illustrative data from an oscilloscope trace of the same photodetector, described above and in FIGs. 7 and 8, illuminated with an adjustable power such that there is a constant 50 mA average photocurrent in the photodetector. That is, the optical power is adjusted slightly to account for the variable quantum efficiency with applied bias in compression. The various curves are for applied bias voltages of 1 2, 3, and 4 Volts. The solid curves are slightly attenuated sinusoids (i.e., attenuated to account for a small amount of expected photodetector and RF transmission losses to the oscilloscope). At 50 mA average (100% modulation depth) photocurrent, the peak load voltage is 2.5 Volts across 50 ohms. FIG. 9 clearly shows the photodetector output being clipped when biased at 1 and 2 volts. While the output is clipped, the photodetector continues to store the charge that is photogenerated during the peak. However, since the photodetector terminal voltage has dropped, space charge compression within the photodetector causes photogenerated carriers to be delayed in being swept through the photodetector. This optionally accounts for the waveform showing wider (in time) sinusoids in the clipped portion of the waveform compared to the ideal (solid) sinusoidal response. At 3 volts, the photodetector output shows a small amount of clipping (although it is a bit difficult to tell). Since the minimum bias from equation (2) is (0.05*50+2*0.05/0.17-0.4) =2.7 Volts, it is easy to see why it may be difficult to see any clipping. At 4 Volts bias, it is clear that the photodetector output is not clipped as the output reaches it's full expected maximum voltage.

An embodiment of the instant invention illustrates ease of scaling to higher frequencies. In this example, a smaller 34 μm diameter (and thus, higher frequency) photodetector processed from the same wafer is also measured. The data for a 34 micron diameter photodetector at 2 GHz is shown in FIG. 10. For this device, the incident light level is fixed at 141 mW and the applied bias voltage is increased from 0 to 6.5 Volts reverse bias as before. The detected photocurrent again varies due to compression at lower applied biases, but at 5V, the detected photocurrent is about 105 mA. At each bias level, the output RF power is measured from the photodetector into the 50 ohm load of an RF power meter. The output RF power is measured and plotted against the total power (optical + electrical) input to the stage. As can be seen in FIG. 26, the output RF power increases with applied bias voltage until total input powers exceed 850 mW. The resulting efficiency peaks at around 42% and decreases to 32% at the highest applied voltage. Again, over this range of applied voltage the photodetector output stage is operating in class AB operation, except for possibly the highest applied voltage.

Nevertheless, efficiencies above 30% have been achieved. The 2 GHz device works from near DC to above 4 GHz.

These photodetectors optionally provide much higher currents. 350 mA small-signal compression currents are measured at bias voltages of 3.5 V (1.2 Watt electric power dissipation potential). It follows that, for example, peak currents under large-signal modulation of over 500 mA are expected with less than 1-dB compression. However, the data above, at 130 mA average currents (260 mA peak currents) in the 100MHz example (FIG. 7), demonstrate that the photodetectors as designed are not optimal for delivering maximum power to a 50 ohm load impedance. An alternative embodiment of the invention for higher voltage operation and lower current provides power delivery to a 50 ohm load. This is accomplished through the redesign of the intrinsic region thickness (slightly thicker) and/or the doping profile within the various semiconductor layers that make up the device.

From the maximum electrical power dissipation observed (1.2 Watts) from this device, an embodiment of the invention optionally includes an output RF power stage providing 500 mW (+27 dBm) from a single device. Other embodiments for photodetectors consistent with the instant invention optionally allow for additional RF power levels from a single photodetector, up to the few Watt level of RF power output.

For narrowband frequency operation, it is possible to adjust parallel impedance 90 and series impedance 80 to yield more optimal performance without a redesign of the internal photodetector structure. This would be similar to the design of an optimal conjugate match for transistor output stages as outlined in S. Cripps, RF Power Amplifiers for Wireless Communications, Artech House Publishers, Norwood MA, 1999, incorporated herein by reference. Specific values of parallel and series impedances 90, 80 are dependent on the specific frequency range of operation or other system needs.

An embodiment of the invention addresses increasing the output voltage of a power photodetector output stage. Fundamentally, the output power stage for a single photodetector design is limited by the maximum electrical power dissipation that is achieved in any power photodetector. While over 2.2 Watts has been achieved (such as described in G.A. Davis, R.E. Weiss, R.A. LaRue, K.J. Williams and R.D. Esman, "A 920-1650 nm High-Current Photodetector," *IEEE Photon. Tech. Lett.*, **8**, pp. 1373, 1996, incorporated herein by reference), which experimentally makes possible the design of a 1 Watt output stage. Extending the power dissipation to the multi-watt level in a single device is difficult, especially for small high frequency devices. Therefore, an embodiment of the invention entailed consideration of single devices constructed into arrays. The embodiment addresses the following problems: achieving higher photocurrent and/or obtaining a single or parallel array of photodetectors that can be biased with sufficient voltage such that load voltage transients do not cause the photodetector terminal voltage to decrease below the minimum required by equation (2), that is, sufficient bias voltage to generate high peak voltages in the output impedance.

To achieve higher voltage operation, an embodiment of the invention, for example, takes advantage of the high shunt resistances that are possible with reversed biased photodetectors and combines the output currents from N series-connected photodetectors 62, 64 as shown in FIG. 11. It is, of course, appreciated that although only two series-connected photodetectors are shown in FIG. 11, other acceptable embodiments of the invention include more than two series series-connected photodetectors. For lumped element operation at low frequencies, the devices can be considered as discrete elements circuit elements as shown in FIG. 12. That is, the photodetectors 62, 64 are represented by ideal current sources 132, 134 of current Ipd, and the internal junction capacitances and the series impedances of the photodetectors are represented as capacitors 142, 144 having capacitances of Cpd, and resistors 152, 154 having resistances of Rpd, as shown in FIG. 12. For this lumped element case, the modulated light is split into N identical outputs (identical in both amplitude and RF phase for identically connected photodetectors) and delivered to N photodetectors (here assumed identical for convenience, but in practice each photodetector's characteristics can be represented individually). In this N-photodetector example, the identical input signals cause the currents to be identical resulting the current Ipd through the load impedance. In this case, it takes N times as much optical power to deliver the same amount of net current to the load impedance. Although this lowers the overall output stage efficiency, it proves useful as it allows N times as much voltage to be delivered to the load due to the applied bias being allowed to be N times the voltage for a single device (that is, 1/N of the applied voltage in this example is dropped across each photodetector). The efficiency equation for an N-element (identical) linear photodetector array connected in series is derived through a similar process that was used to arrive at equation (2). The N-photodetector efficiency is:

$$\eta = \frac{1}{\left(2 + \frac{4N}{\alpha R} + \frac{2NV_{th}}{V_{pk-load}} + \frac{NP_{abs}}{P_{load}}\right)} \qquad (4)$$

where Pabs is the power absorbed by a single photodetector. Equation (4) is plotted in FIG. 13 for N=1, 4 and 8 (again with alpha being infinite and Vth = 0). Despite the seemingly obvious inefficiency of having to deliver N times the optical power to yield the same load photocurrent as the single photodetector output stage, the efficiency that is obtainable is quite good. Even for RF output powers near 1 Watt, over 30% efficiency is possible in an embodiment of the invention. In fact, in an embodiment of the invention, if a single photodetector is capable of 1 Watt electrical power dissipation and 1/2 watt output RF power, then an N = eight element series connected array of the same photodetectors are capable of 8 Watts electrical power dissipation and up to 4 Watts of RF power output at up to 36% efficiency. The peak efficiency still approaches 50% as the RF power increases, even for the N-element array. This is due to the fact that the NPabs/Pload term in equation (3) is proportional to 1/Vload because Pabs is proportional to Iload and Pload is proportional to Iload*Vload. As Vload increases, this term in equation (3) naturally decreases in importance and becomes a smaller contribution to the overall efficiency degradation. This suggests that there is a balance to be determined in the number of photodetectors required to achieve a given output RF power versus the desired efficiency needs and the individual photodetector capabilities.

The factor of N in the term containing alpha should not be overlooked. The increase in N in this term will degrade efficiency since this is a significant term for high power photodetectors. This term will limit the efficiency that is obtainable. Increasing alpha is complicated. However, alpha is fundamentally limited by the series impedance Rpd in the photodetector as well as by space charge effects. In fact, for the photodetectors used in the single photodetector output stage discussed above, the series impedance (for example, about 6 ohms from forward IV measurements) is solely responsible for alpha since the upper limit for alpha is 1/Rpd (1/6 =0.167), near where these photodetectors presently are.

For lumped element parallel connected photodetectors, the RC limited bandwidth is reduced due to the larger capacitance (parallel capacitors add). See, e.g., K.J. Williams and R.D. Esman, "Large-Signal Compression-Current Measurements in High-Power Microwave p-i-n Photodiodes," *Electronics Lett.*, vol. 35, no. 1, pp. 82-84, Jan 1999, incorporated herein by reference. For series-connected photodetectors, the bandwidth should actually increase due to the series combination of capacitance resulting in lower net capacitance. Referring to the equivalent circuit diagram of FIG. 12, the ratio of output current to input current is given by:

$$\frac{i_{load}}{i_{pd}} = \frac{1}{\left(1 + j\frac{\omega R_L C_{pd}}{N} + j\omega R_{pd} C_{pd}\right)} \qquad (5)$$

When identical photodetectors are assumed. As compared to the single photodetector ratio which is given by:

$$\frac{i_{load}}{i_{pd}} = \frac{1}{\left(1 + j\omega R_L C_{pd} + j\omega R_{pd} C_{pd}\right)} \qquad (6)$$

The equations are similar and are equivalent when the capacitance in the single photodetector equation is replaced by Cpd/N for an N-element series array. The 3-dB frequency (that is, the frequency at which the response decreases by 3-dB) of the single photodetector is proportional to 1/Cpd, thus the 3-dB frequency of the series-connected array is N times higher that in the single photodetector case when Rpd<<RL.

To verify this bandwidth enhancement a series connected pair (N=2) of RC limited photodetectors were connected in a manner similar to FIG. 11. To prevent voltage drift of the individual detector voltages, an embodiment of the invention provides a bias to the connection between the two photodetectors. An illustrative diagram for this embodiment of the invention is shown in FIG. 14, showing a voltage biases 45, 47. This embodiment of the invention prevents voltage drift due to the "floating" connection between the photodetectors. This embodiment of the invention is useful when the shunt resistance of the detectors is high, causing excessively slow voltage drift and/or alternatively excessively long voltage equilibrium times. The shunt resistance in parallel with the ideal current source is not shown in the equivalent circuit diagrams because it is high and rarely affects the RF performance in 50 ohm systems. A high impedance (that is, high impedance relative to the 50 ohm output load impedance) biasing ladder network or other bias supply network could have alternatively been used to keep the number of voltage sources to one, even for an N-series connected array. This particular biasing implementation does not appreciably affect the efficiency. The frequency response for two series-connected photodetectors (identically illuminated) is plotted in FIG. 15 along with the frequency response of the two photodetectors when they are measured individually. The frequency response increases throughout the region where the photodetectors naturally roll off individually exactly as equation (5) suggests since the photodetector's 3-dB bandwidth increased from 600 MHz to 1.2 GHz.

The aforementioned series-connected photodetector arrays are analyzed with lumped-element circuit analysis. As frequencies increase and the electrical distance separation between the furthest two detectors approaches a fraction of the RF wavelength, this approach is no longer valid. In this case traveling wave designs have to be considered because the RF energy from each photodetector will not add up in phase at the output load impedance. In an embodiment of the invention, the RF phase of the incoming light waves is modified. However, such modification may perturb the result slightly due to the impedance mismatches. An alternate embodiment of the invention includes imbedding the photodetectors in a transmission line with matching impedances and adjusting the incoming lightwave phases such that the output currents add properly while maintaining a good transmission line impedance match with the output load impedance. This is a natural high frequency extension of the lumped element series combination from above. An example of such an N=3 photodetector configuration is shown in FIG. 16 where L / C are biasing inductors/capacitors as before. The bias voltages or bias network is designated by block 49. The electrical distance between the photodetectors is adjusted along with the modulated light delivery fiber lengths (RF phase) such that the reverse photocurrents, Irev, add up in phase. Series and parallel impedances 80, 90 of Zs and Zp are needed and their values are chosen to create a characteristic impedance for the transmission line that matches the load impedance Zload. A reverse match 160 having impedance Zm, is used in an embodiment of the invention to limit ripple in the frequency response. This formulation has a distinct and enabling feature for high RF power: the configuration in FIG. 16 allows for higher voltage operation (just as in the lumped element design) in contrast to traveling wave or array designs wherein current scaling is the focus. Here again N is optionally arbitrarily large if the series resistive losses can be made small.

Another embodiment of the invention combines current scaling attributes with the series combinations of photodetectors for voltage scaling. This embodiment involves two types of scaling: a two dimensional array of a single-ended design and/or one or two dimensional arrays implemented in a balanced output configuration. The two types are implemented either in a lumped element or in a traveling wave design, depending on the frequency range of interest.

A parallel combination of photodetectors, by itself, to accomplish current scaling for high power output stages suffers from the limited voltage operation of single photodetectors. In fact, it is now possible to exceed the voltage limits with a single photodetector as outlined above. If however, the series combination of photodetectors is used, the penalties associated with scaling the voltage are small. While the efficiency is degraded slightly, the bandwidth of the series combination actually improves due to the series combination of capacitors (leading to lower total capacitance). Therefore, it should be possible to do further scaling of the output RF power through the combination of both voltage and current scaling. FIG. 17 shows a diagram of an illustrative lumped element implementation of a N x M (N=number of series connected photodetectors 160 & M=number of parallel N-series combinations 170) array. Thus, the array consists of NxM photodetectors. If the fiber feeds to each photodetectors are RF phase-matched, all NxM signals combine coherently at the load impedance. The efficiency of the NxM array of devices is:

$$\eta = \frac{1}{\left(2 + \frac{4N}{\alpha RM} + \frac{2NV_{th}}{V_{pk-load}} + \frac{NMP_{abs}}{P_{load}}\right)} \quad (7)$$

where Pabs here is the power absorbed in a single photodetector in the array. Thus the total optical power required for the array is N x M x Pabs. With the addition of parallel combinations of series-connected photodetectors, the efficiency actually improves over the N-series connected structure of FIG. 11. This is due to the last term in the denominator being the same as in equation (6) because Pload also increases by M. (This is a consequence of how Pabs is defined). Therefore, the increase in efficiency comes from the second term in the denominator, which is reduced because of the reduction of the importance due to series losses. The addition of additional series-connected detectors in parallel causes the total series resistance to reduce (resistors in parallel lower the total resistance).

The bandwidth of the NxM structure is a combination of the bandwidth enhancing properties of the series-connected detectors and the bandwidth reducing properties of the parallel-connected detectors. In fact, if the detector series impedance is neglected, the bandwidth of an NxN array of identical detectors should be the same and the bandwidth of a single detector. If the power dissipation in each single detector can be made as high as 2 watts (already demonstrated) which allows for a 1 watt output RF power when optimally designed for 50 ohms, then the power dissipated from a N x M array is 2 x N x M Watts, yielding a N x M Watts RF output power potential. For N = M = 8, this yields RF output powers of 64 Watts. Higher output powers are possible with this array concept since N and M could be even larger than 8. It is worth noting here that an 8x8 array providing 64 Watts would require less than 14 Watts of optical power (assuming high quantum efficiency) with the remainder of "power" coming from the voltage bias supply. The optical power needed to supply the array of photodetectors in such a system is well within the realm of, for example, current erbium fiber amplifier technology.

With the possibility to extend the voltage output using series connected photodetector arrays, this also then enables high output power balanced photodetector arrays configured for high output power operation. A balanced high current detector differential pair causes the applied voltage necessary across both photodetectors to be twice that of the single photodetector due to the higher voltage transient across the load. FIG. 18 shows an illustrative, lumped element configuration for a balanced differential output stage requiring two N x M arrays of photodetectors, where N, M greater than or equal to 1. The balanced configuration will allow not only for high output RF powers, but also the noise balancing properties of differential pairs will be useful as has already been demonstrated in lower power configuration. This may help to reduce the noise figure of an embodiment of the invention, should the intensity noise be a significant contributor to the overall amplifier noise figure. The extension of both the N x M lumped element array (shown by way of example in FIG. 17) and the balanced N x M lumped element array (shown by way of example in FIG. 18) to traveling wave designs is an option for higher frequency operation.

Although for ease of understanding, the term photodetector has been used above, it is to be understood that the invention includes embodiments using any acceptable optically controlled current sources. Examples of acceptable optically controlled current sources for use in implementing embodiments of the instant invention include photodetectors with high current capability such as discussed above, photoconductive switches such as Austin switches, and avalanche photodiodes. 10kHz-1THz.

Although the above description of the invention specifically mentions RF, it is to be understood that alternate frequency ranges are acceptable. For example, an acceptable frequency range is between DC (0 Hz) and 100s of THz. The upper limit of the frequency range depends on the frequency response of the Optical-to-RF converters 10 and the frequency response of the RF-to-Optical converters 30.

Because numerous modifications and variations of the above-described invention will occur to those of ordinary skill in the art, it is not desired to limit the invention to the exact construction and operation illustrated and described. Accordingly, all suitable modifications and equivalents may be resorted to, falling within the scope of the invention.

What is claimed is:

1. An apparatus comprising:

an impedance matching circuit;

a biasing circuit; and

a plurality of serially connected optically controlled current sources for detecting amplitude-modulated light at RF frequencies, said plurality of serially connected optically controlled current sources connected to said impedance matching circuit and to said biasing circuit.

2. The apparatus according to claim 1, further comprising: a plurality of voltage drift prevention circuits connected said plurality of serially connected optically controlled current sources.

3. The apparatus according to claim 2, wherein the biasing circuit comprises a bias voltage, and each voltage drift prevention circuit of said plurality of voltage drift prevention circuits comprises an inductor and a fractional voltage of said bias voltage connected thereto.

4. The apparatus according to claim 3, wherein said biasing circuit applies a respective bias voltage to each optically controlled current source of said plurality of serially connected optically controlled current sources.

5. The apparatus according to claim 2, wherein said biasing circuit comprises a plurality of passive electrical components.

6. The apparatus according to claim 1, further comprising a transmission line imbedded in which are said plurality of optically controlled current sources; and a plurality of impedances corresponding to each of said plurality of optically controlled current sources.

7. The apparatus according to claim 1, further comprising at least one of a laser and an optical amplifier communicating with said plurality of serially connected optically controlled current sources.

8. The apparatus according to claim 1, wherein each of said plurality of optically controlled current sources comprises at least one of a photodetector, a photoconductive switch, and an avalanche photodiode.

9. An apparatus comprising:

an impedance matching circuit;

a biasing circuit; and

a plurality of parallel, optically controlled current source arrays, each optically controlled current source array of said plurality of parallel, optically controlled current source arrays being connected to said impedance matching circuit and to said biasing circuit, said each optically controlled current source array of said plurality of parallel, optically controlled current source arrays comprising a plurality of serially connected optically controlled current sources for detecting amplitude-modulated light at RF frequencies.

10. The apparatus according to claim 9, further comprising: a plurality of voltage drift prevention circuits connected said plurality of serially connected optically controlled current sources.

11. The apparatus according to claim 10, wherein the biasing circuit comprises a bias voltage, and each voltage drift prevention circuit of said plurality of voltage drift prevention circuits comprises an inductor and a fractional voltage of said bias voltage connected thereto.

12. The apparatus according to claim 11, wherein said biasing circuit applies a respective bias voltage to each optically controlled current source of said plurality of serially connected optically controlled current sources.

13. The apparatus according to claim 10, wherein said biasing circuit comprises a plurality of passive electrical components.

14. The apparatus according to claim 9, further comprising a transmission line imbedded in which are said plurality of optically controlled current sources; and a plurality of impedances corresponding to each of said plurality of optically controlled current sources.

15. The apparatus according to claim 9, further comprising at least one of a laser and an optical amplifier communicating with said plurality of serially connected optically controlled current sources.

16. The apparatus according to claim 9, wherein each of said plurality of optically controlled current sources comprises at least one of a photodetector, a photoconductive switch, and an avalanche photodiode.

17. An apparatus comprising:

a first impedance matching circuit;

a first biasing circuit; and

a first plurality of parallel, optically controlled current source arrays, each optically controlled current source array of said first plurality of parallel, optically controlled current source arrays being connected to said first impedance matching circuit and to said biasing circuit, said each optically controlled current source array of said first plurality of parallel, optically controlled current source arrays comprising a first plurality of serially connected optically controlled current sources for detecting amplitude-modulated light at RF frequencies;

a second biasing circuit comprising an opposite voltage polarity relative to said first biasing circuit; and

a second plurality of parallel, optically controlled current source arrays connected to said first impedance matching circuit, each optically controlled current source array of said second plurality of parallel, optically controlled current source arrays being connected to said first impedance matching circuit and to said biasing circuit, said each optically controlled current source array of said second plurality of parallel, optically controlled current source arrays comprising a second plurality of serially connected optically controlled current sources for detecting amplitude-modulated light at RF frequencies.

18. The apparatus according to claim 17, further comprising: a plurality of voltage drift prevention circuits connected said plurality of serially connected optically controlled current sources.

19. The apparatus according to claim 18, wherein the biasing circuit comprises a bias voltage, and each voltage drift prevention circuit of said plurality of voltage drift prevention circuits comprises an inductor and a fractional voltage of said bias voltage connected thereto.

20. The apparatus according to claim 19, wherein said first biasing circuit applies a respective bias voltage to each optically controlled current source of said first plurality of serially connected optically controlled current sources, and said second biasing circuit

applies a respective bias voltage to each optically controlled current source of said second plurality of serially connected optically controlled current sources.

21. The apparatus according to claim 18, wherein said biasing circuit comprises a plurality of passive electrical components.

22. The apparatus according to claim 17, further comprising a transmission line imbedded in which are said plurality of optically controlled current sources; and a plurality of impedances corresponding to each of said plurality of optically controlled current sources.

23. The apparatus according to claim 17, further comprising at least one of a laser and an optical amplifier communicating with said plurality of serially connected optically controlled current sources.

24. The apparatus according to claim 17, wherein each of said plurality of optically controlled current sources comprises at least one of a photodetector, a photoconductive switch, and an avalanche photodiode.

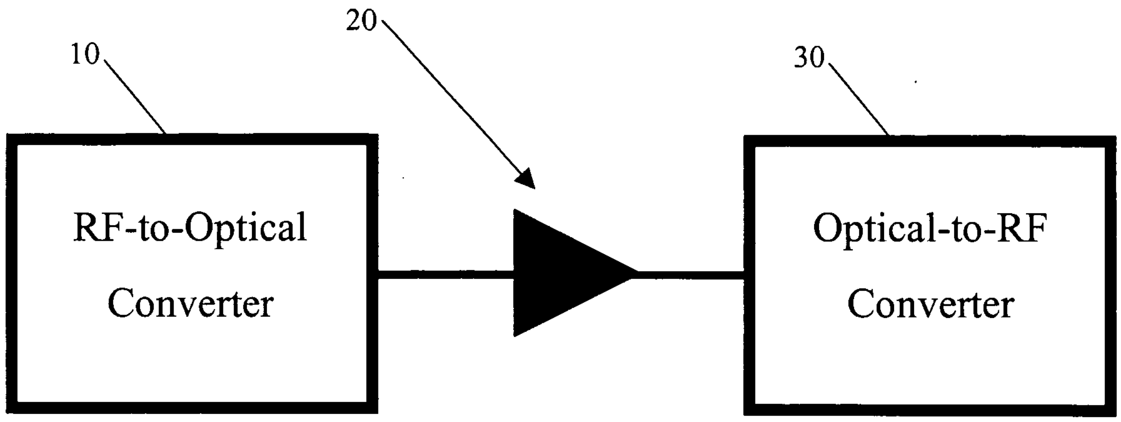
10
20
30
RF-to-Optical
Converter
Optical-to-RF
Converter

FIG. 1

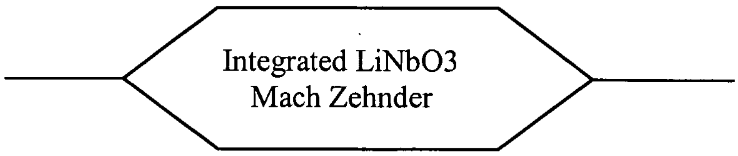
Integrated LiNbO3
Mach Zehnder

FIG. 2

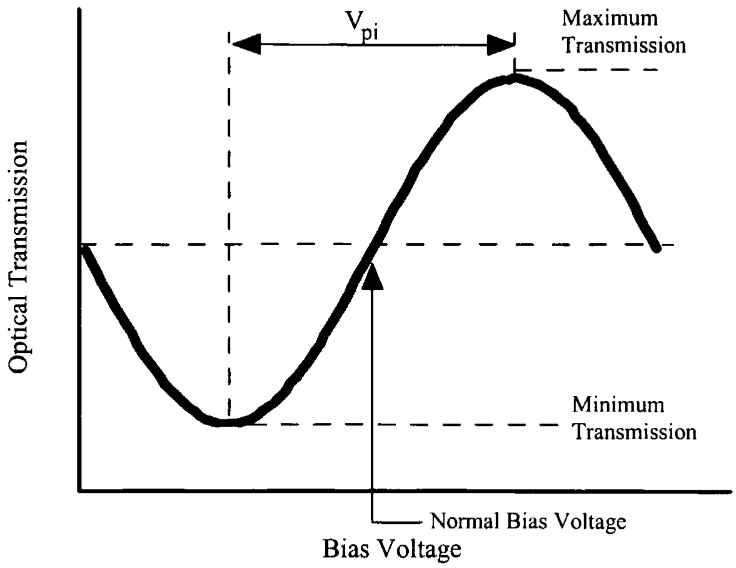

FIG. 3

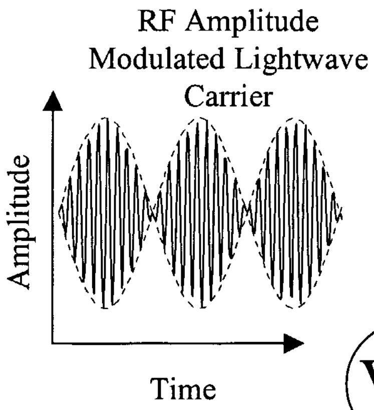

FIG. 4a

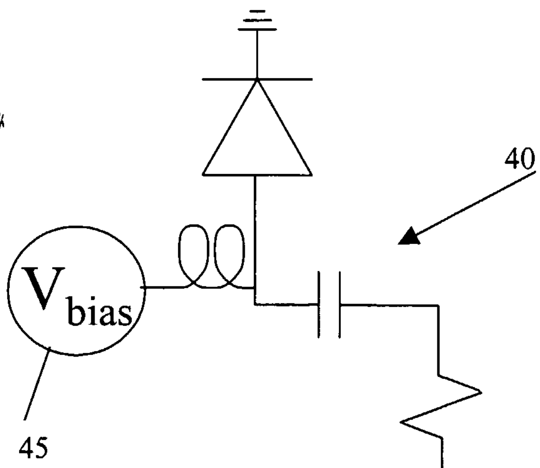

FIG. 4b

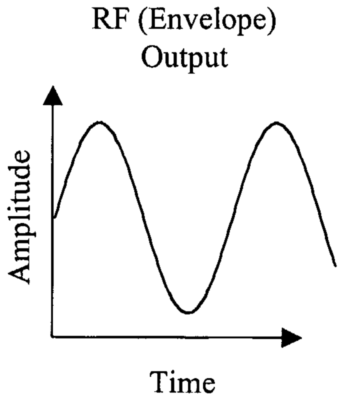

FIG. 4c

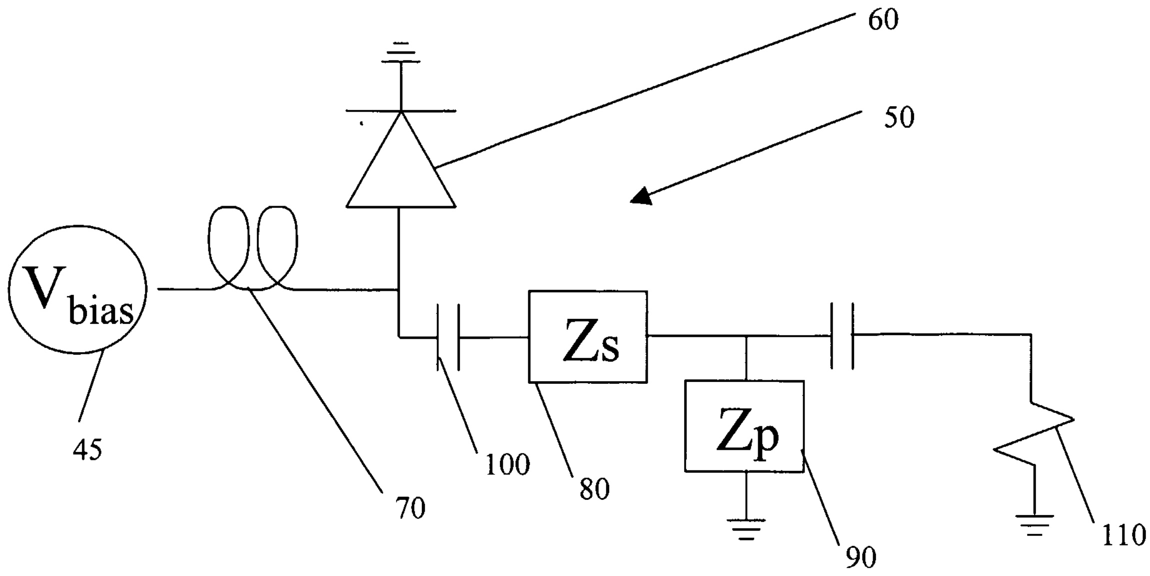
60
50
V_{bias}
Zs
Zp
45
70
100
80
90
110

FIG. 5

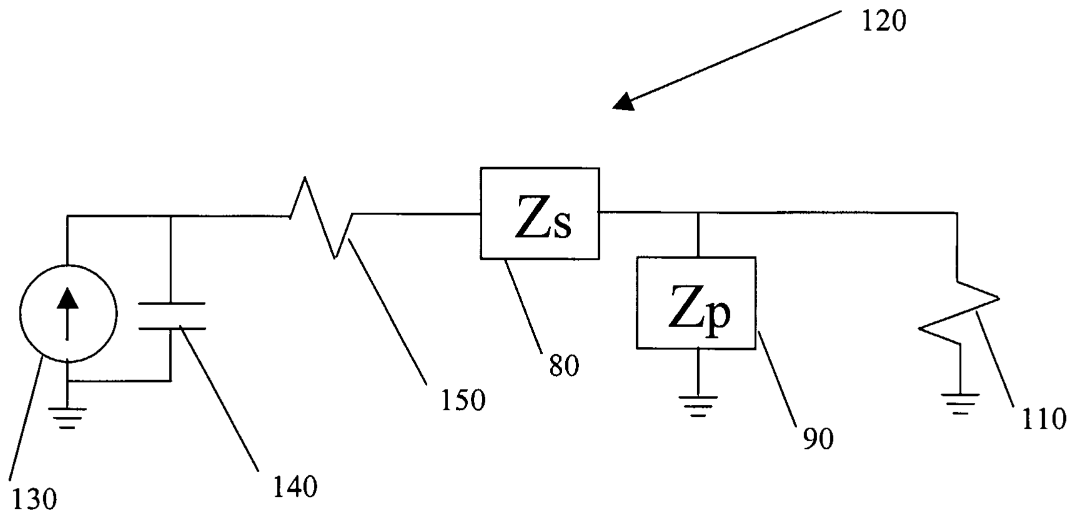
120
Zs
Zp
150
80
90
110
130
140

FIG. 6

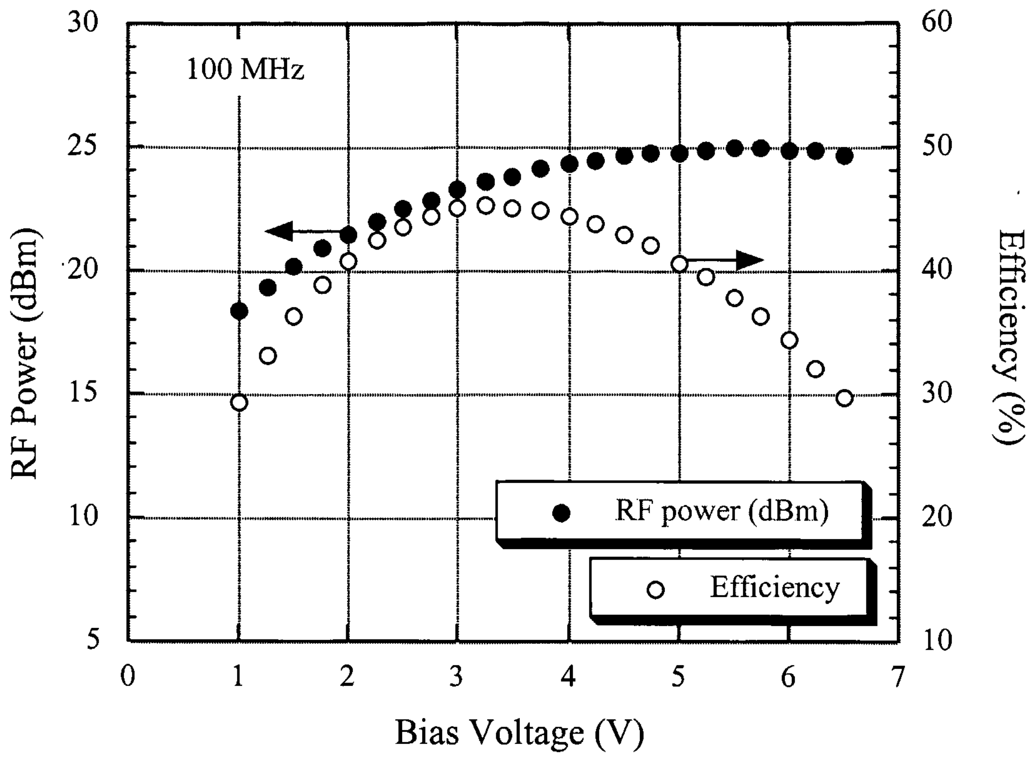
100 MHz
RF Power (dBm)
Efficiency (%)
Bias Voltage (V)
RF power (dBm)
Efficiency
30
25
20
15
10
5
60
50
40
30
20
10
0
1
2
3
4
5
6
7

FIG. 7

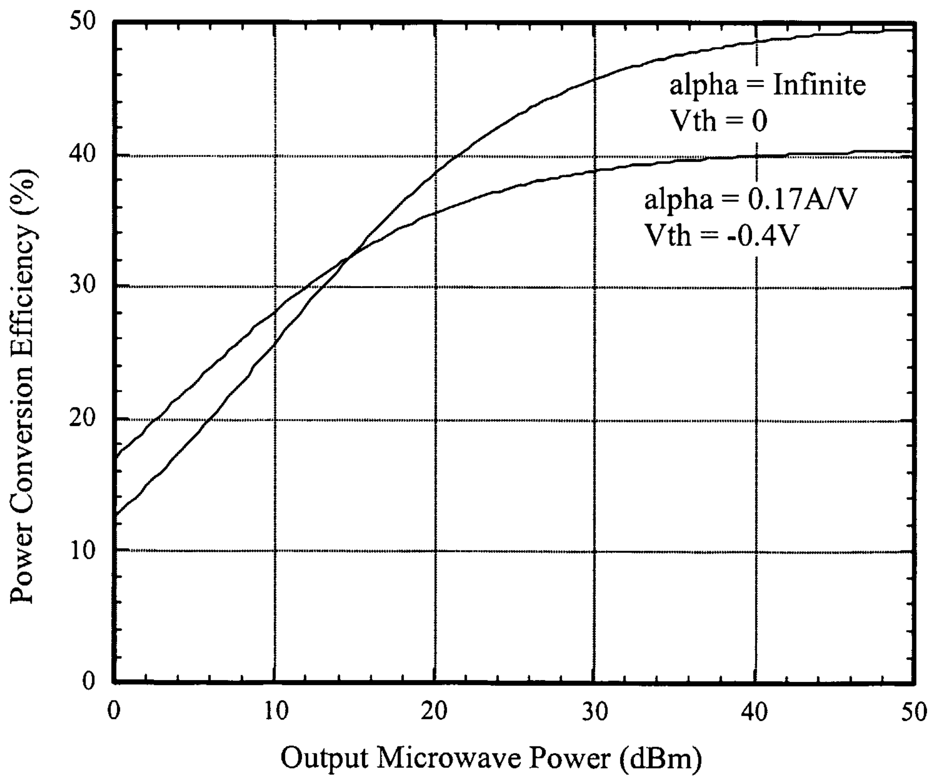
Power Conversion Efficiency (%)
Output Microwave Power (dBm)
alpha = Infinite
Vth = 0
alpha = 0.17A/V
Vth = -0.4V
50
40
30
20
10
0
0
10
20
30
40
50

FIG. 8

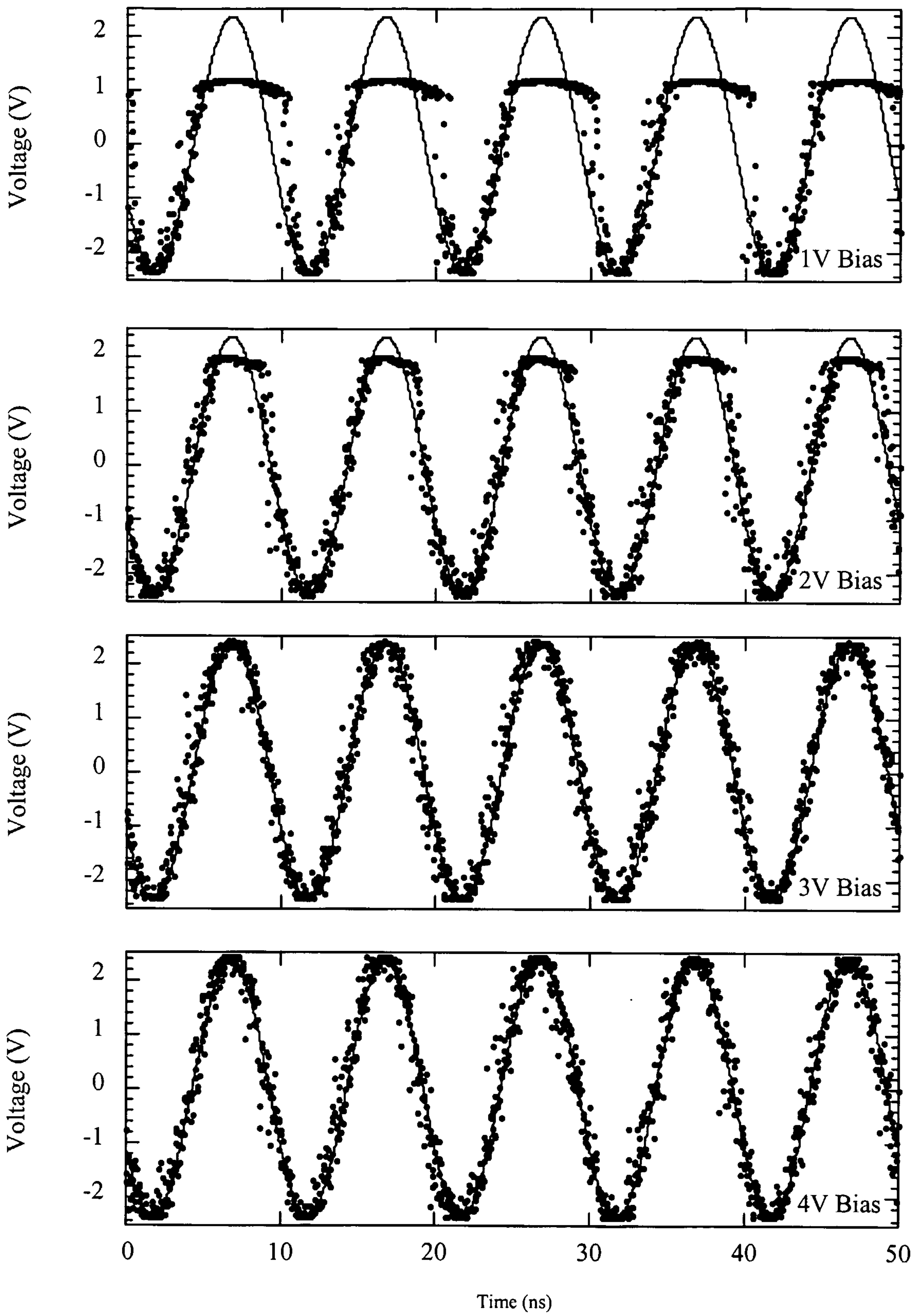
Voltage (V)
2
1
0
-1
-2
1V Bias
2V Bias
3V Bias
4V Bias
0
10
20
30
40
50
Time (ns)

FIG. 9

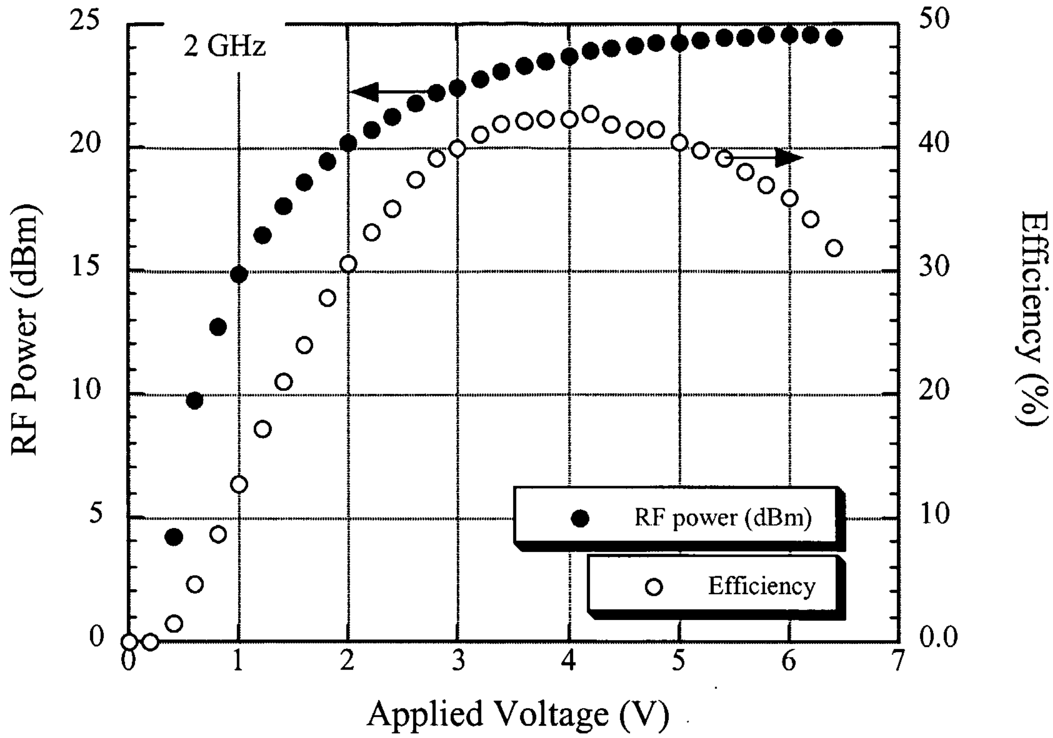
2 GHz
RF Power (dBm)
Efficiency (%)
Applied Voltage (V)
RF power (dBm)
Efficiency
25
20
15
10
5
0
50
40
30
20
10
0.0
0
1
2
3
4
5
6
7

FIG. 10

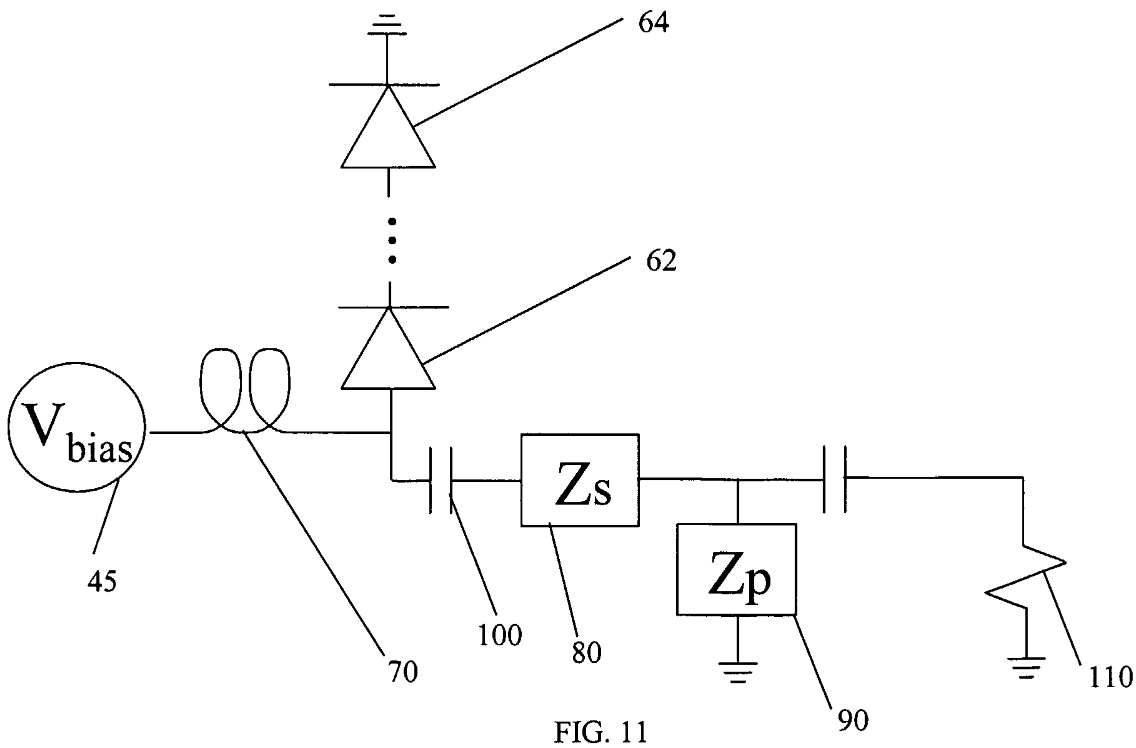
64
62
Vbias
Zs
Zp
45
70
100
80
90
110

FIG. 11

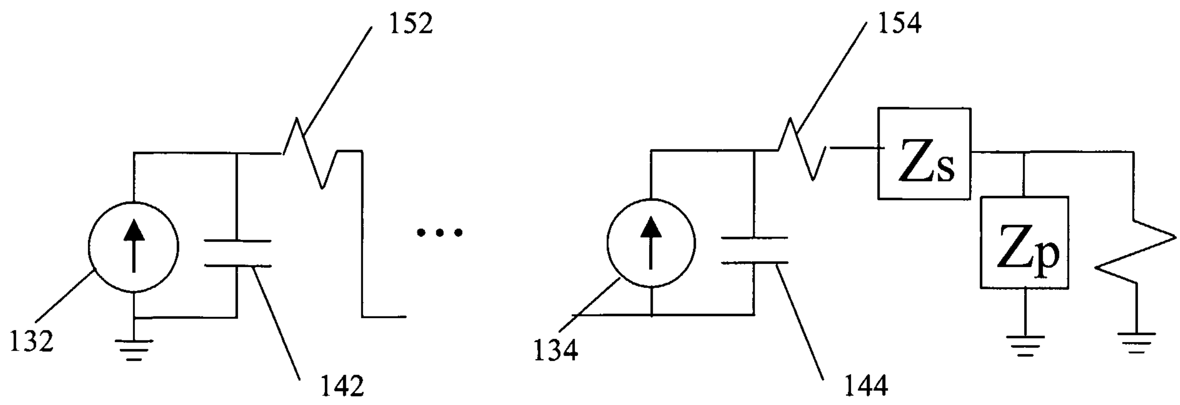
152
154
Zs
Zp
132
142
134
144

FIG. 12

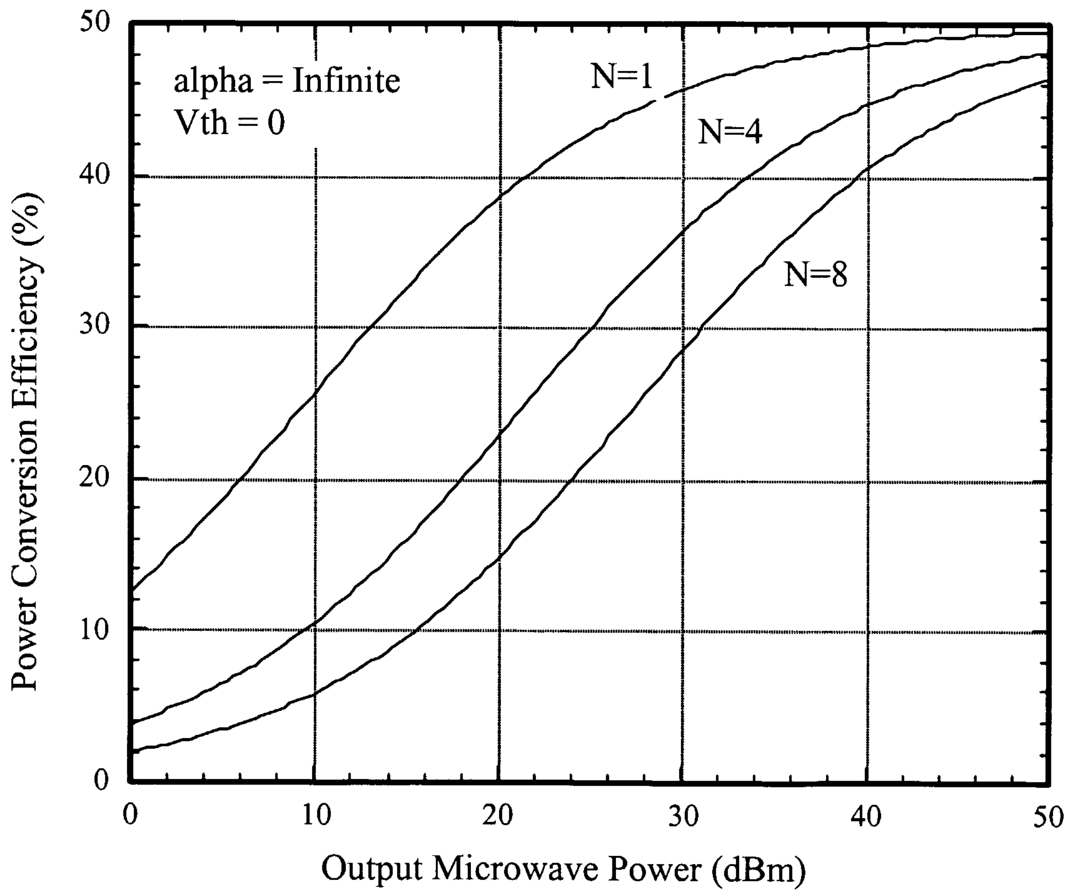
alpha = Infinite
Vth = 0
N=1
N=4
N=8
Power Conversion Efficiency (%)
Output Microwave Power (dBm)
0
10
20
30
40
50

FIG. 13

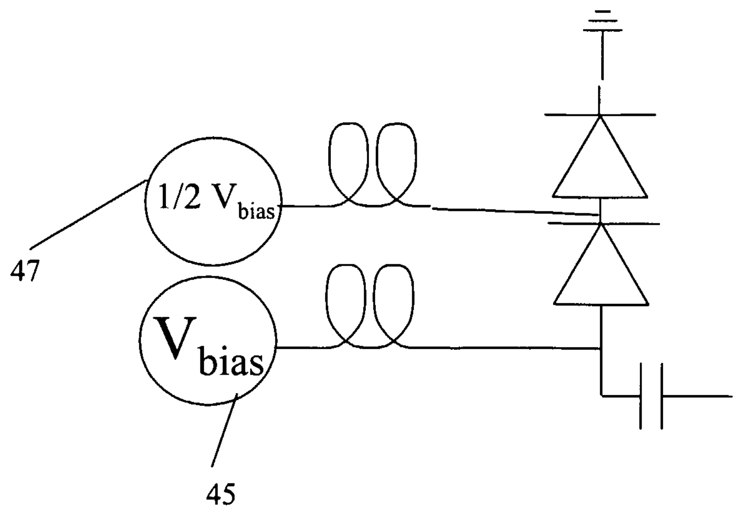
1/2 V bias
V bias
47
45

FIG. 14

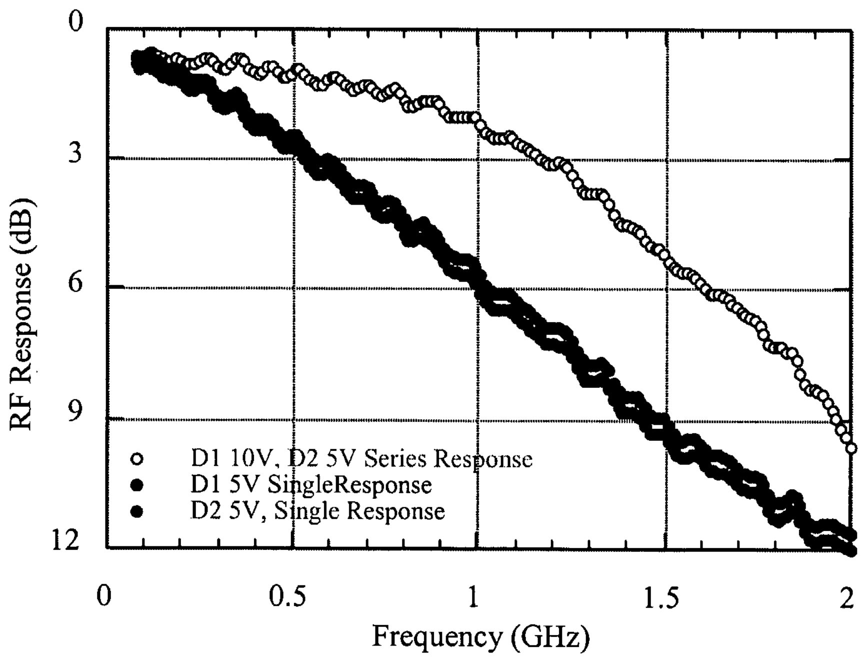
RF Response (dB)
0
3
6
9
12
0
0.5
1
1.5
2
Frequency (GHz)
D1 10V, D2 5V Series Response
D1 5V SingleResponse
D2 5V, Single Response

FIG. 15

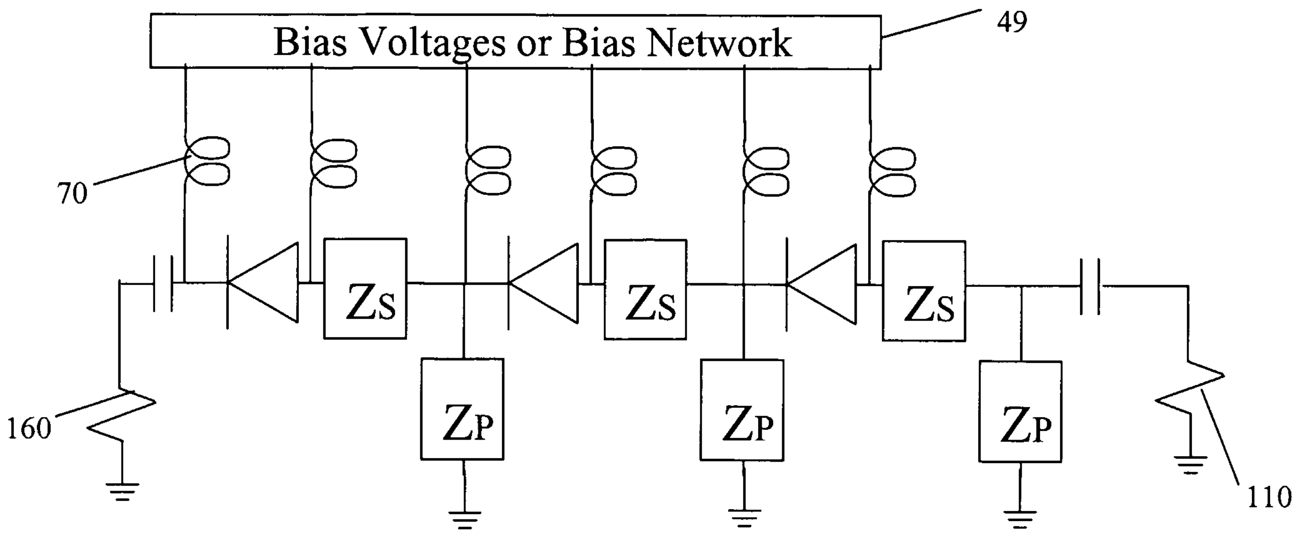
Bias Voltages or Bias Network
49
70
160
Zs
Zs
Zs
Zp
Zp
Zp
110

FIG. 16

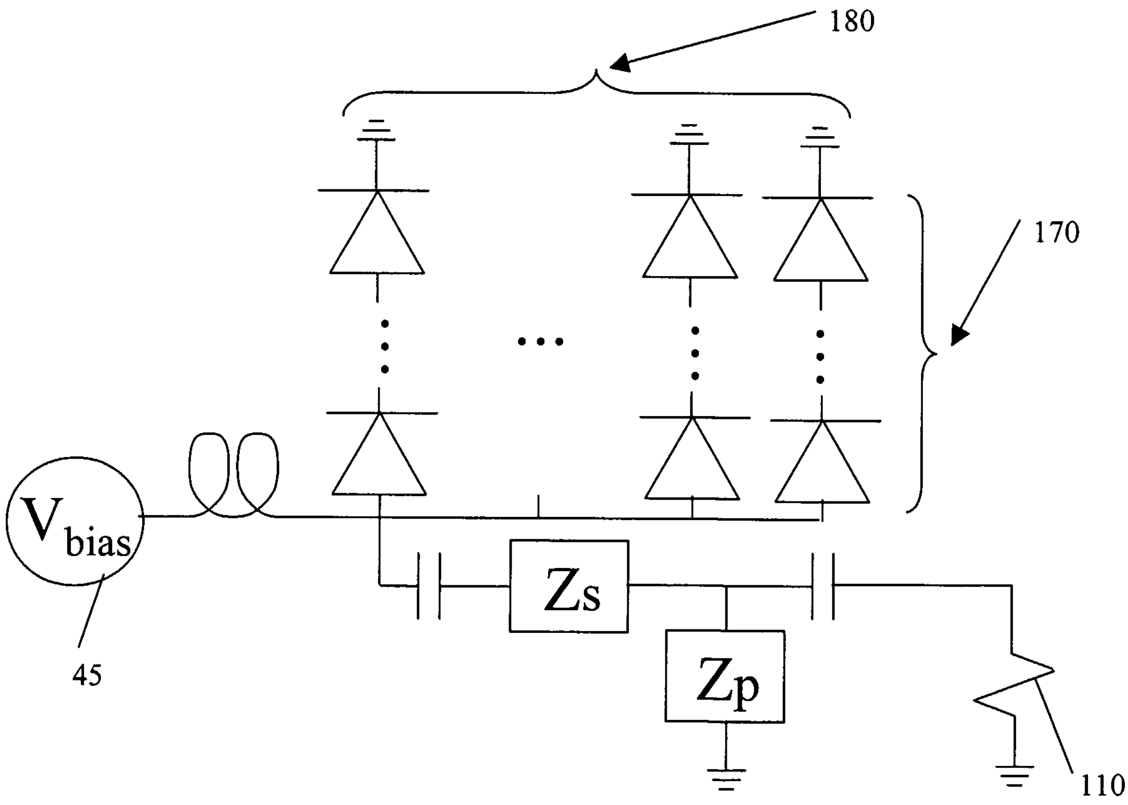
180
170
Vbias
45
Zs
Zp
110

FIG. 17

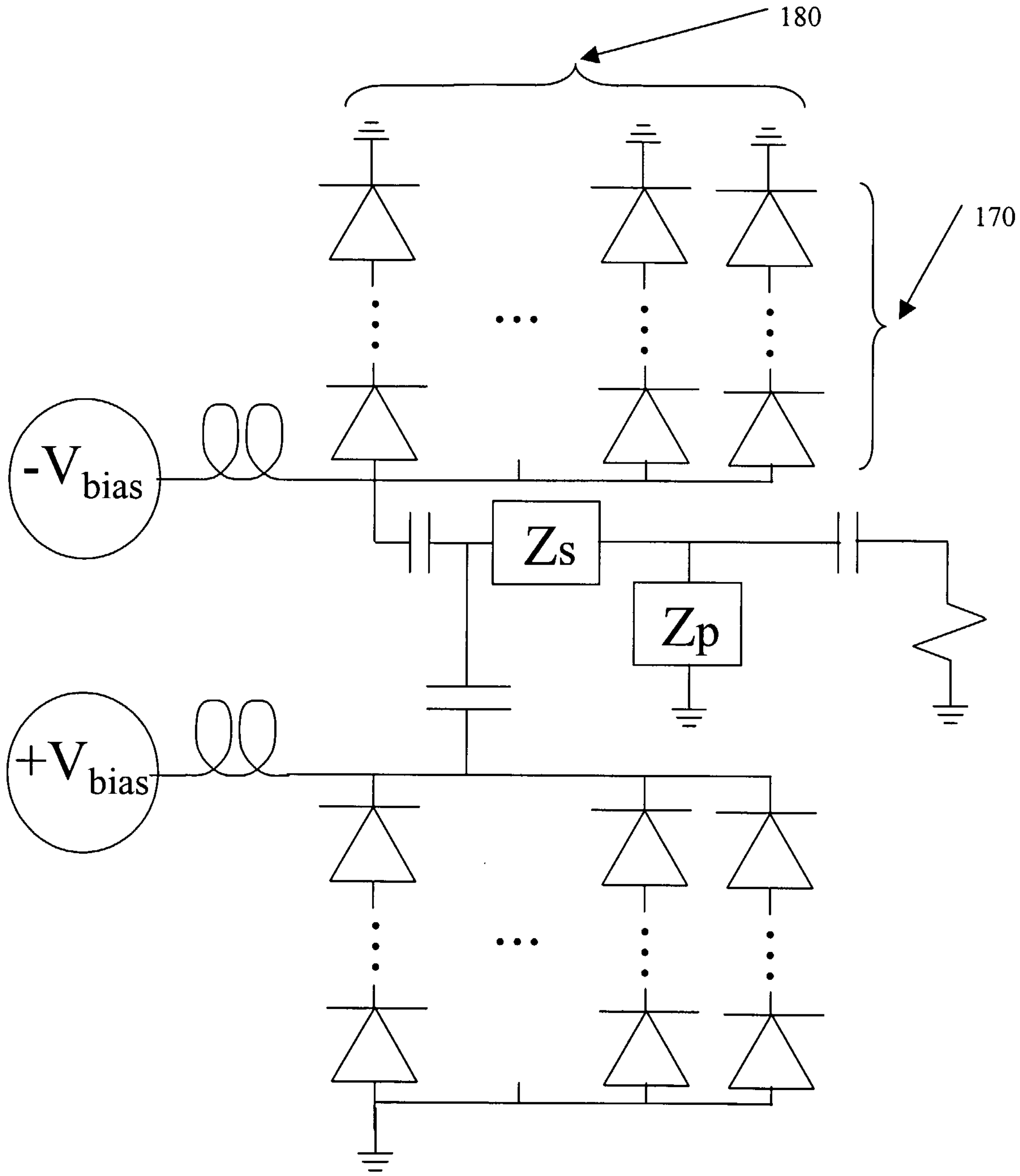

FIG. 18